International Journal of Advanced Research in Biological Sciences
ISSN: 2348-8069
www.ijarbs.com
Volume 3, Issue 6 - 2016

Research Article

SOI: http://s-o-i.org/1.15/ijarbs-2016-3-6-32

Structural investigation, biological and flotation studies of Co(II) and Zn(II) complexes of salicoyl hydrazone ending by thiazole ring.

Magdy M. Khalifa[1], Hany M. Youssef[1], Abdulnasir A. Majeed[1], Gaber M. Abu El-Reash[1*]

[1]Department of Chemistry, Faculty of Science, Mansoura University, Mansoura, Egypt.
* Corresponding author.: **Prof. Dr. Gaber Mohammed Abu El-Eeash**
Tel.: +201000373155; fax: +20 502219214.
E-mail address: gaelreash@mans.edu.eg

Abstract

Co(II) and Zn(II) complexes derived from hydrazone ligand (H_2STH) prepared via the condensation of 2-amino -4-yl aceto thiosemicarbazide to 2-hydroxybenzaldehyde (salicylaldehyde) were synthesised and characterized using elemental analysis, magnetic and spectral measurements. The proposed structures of both complexes were proved using DFT optimization and conformational analysis. The thermal decomposition behaviour of both complexes were discussed. Kinetic parameters (ΔH, ΔS, ΔG, E and A) of resulted thermal decomposition stages have been calculated using Coats-Redfern and Horowitz-Metzger methods. Ion-flotation separation of Zn(II) ions was carried out from aqueous solutions using oxime derivative as chelating agent and oleic acid as surfactant. Co(II) complex shows the highest Cytotoxicity activity and minimum inhibitory concentration (MIC) activity against *Staphylococcus aureus*, *Escherichia coli* and *Candida albicans*.

Keywords: Hydrazones; Spectral characterization; thermal degradation; Ion-flotation separation; Cytotoxicity activity.

Introduction

An important role of thiosemicarbazons being NNS and NSO tridentate donors had carcinomatotic influence [1] and substantial in vivo activity versus different human tumor lines [2, 3] but the structural variations of some thiosemicarbazides owing to chelating ability may damage or reduce its medicinal properties [4]. Also thiosemicarbazons used as reagents for analysis of metals [5-7], device applications relative to telecommunications and optical storage [8, 9] In addition to our earlier work [10, 11], the present work aims to synthesize and characterize Co(II) and Zn(II) complexes of (E)-2-(2-aminothiazol - 4-yl) - N'- (2-hydroxybenzylidene) acetohydrazide (H_2STH). The modes of chelation and the geometry of complexes are discussed relies on the obtained (DFT) quantum calculations and the magnetic moment measurements, The different spectroscopic data (^{1}H and ^{13}C-NMR, IR, UV-visible). Moreover, the thermal behavior of the degradation stage and its kinetic parameters have been discussed by employing Coats–Redfern and Horowitz–Metzger models. Also, (H_2STH) used in removal of Zn(II) from aqueous solutions in an effective manner using ion flotation method. Ion flotation as an extraction technique has lately gained a significant attention because its rapidity, simplicity good separation yields (R > 95 %) for small concentrations (10^{-6}–10^{-2} mol.L^{-1}) of pollutants, and numerous applications for species having different structure and nature and finally easiness of processing for recovery purpose [12].

Therefore, the flotation technique was chosen for this investigation. Ion flotation includes the removal of metal ions from aqueous solutions using surfactants which act as collectors. Also, it aims to develop a simple, rapid and effective method for the pre-concentration and determination of Zn(II) using ion flotation technique in aqueous solutions using (H_2STH) derivative as complexing agent and oleic acid (HOL) as surfactant. For this regard, the effect of different parameters including, pH, surfactant, metal ions and ligand concentrations, were optimized. Also their Minimum inhibitory concentration (MIC) and Cytotoxicity assay have been tested.

Experimental

Materials and Instrumentation.

The Co(II) and Zn(II) chloride salts, ethyl 2-(2-aminothiazol-4-yl)acetate, hydrazine hydrate and 2-hydroxy benzaldehyde (salicylaldehyde) were of analytical grade. Oleic acid (HOL) surfactant stock solution 6.36×10^{-2} mol L^{-1}, was prepared by dispersing 20 mL in one liter of kerosene. Zinc chloride ($ZnCl_2$) stock solution, 1×10^{-2} mol L^{-1}, was prepared in double distilled water. The stock solution of H_2STH, 1×10^{-2} mol L^{-1}, was prepared in absolute ethyl alcohol. (C, H and N) percent in the prepared H_2STH and complexes were detected using a Perkin–Elmer 2400 series II analyzer, while metal and chloride contents were carried out according to the standard methods [13]. Thermogravimetric (TGA) and differential thermal analysis (DTA) measurements were carried out on a Shimadzu TGA-50H thermogravimetric analyzer at temperature range (20–800°C) with a heating rate of 10 ^{o}C/min and nitrogen flow rate of 15 ml/min. The standard used in the experiment is Pt. 10% Rh. A Sherwood Magnetic Balance was utilized to measure the magnetic susceptibility of solid complexes. IR spectra were recorded on a Mattson 5000 FTIR spectrophotometer in range (4000–400 cm^{-1}) using KBr discs, while Perkin Elmer Lamda 25 UV/Vis Spectrophotometer was used to record the electronic spectra of complexes in DMSO solution. ^{1}H and ^{13}C-NMR measurements in d_6-DMSO at room temperature were carried out on Mercury and Gemini 400 MHZ spectrometer. In ion-flotation separation of Zn(II) ions, All the determinations of the analytes were carried out using GBC, Sensaa Series Atomic Absorption Spectrometry (computerized AAS) with air-acetylene flame under the optimum instrumental conditions. The flotation and separation cells were a glass cylinder with 45 cm length and 6 cm inner diameter with a quick-fit stopper at the top and a stopcock at the bottom [14]. These cells were used to examine the separation of Zn(II) ions from 1 L of some natural water samples. The pH of studied solutions was adjusted using Hanna Instrument 8519 digital pH meter.

Synthesis of H_2STH

2-(2-aminothiazol-4-yl)acetohydrazide was prepared by refluxing hydrazine hydrate and 2-(2-aminothiazol-4-yl)acetate in absolute hot ethanol for 1 hr. then the resultant material filtered, washed with hot absolute ethanol and dried in air. Known amount of resultant material mixed with 2-hydroxy benzaldehyde (salicylaldehyde) and the mixture was refluxed on a water bath for a time of (2-4 hours). The condensation product washed and crystallized several times from absolute ethanol and dried in a vacuum desiccator over anhydrous $CaCl_2$. (M.p 205 ^{o}C).

Synthesis of Complexes

All complexes were obtained by mixing the hot ethanolic solution of both the respective metal chloride (1.0 mmol) and H_2STH (1.0 mmol). The mixture was boiled under reflux for 3– 4 h. All products were filtered off, then washed well with hot EtOH followed by diethyl ether. The elemental analysis and physical data of both H_2STH and its complexes are listed in (Table 1). All prepared complexes are stable in air and have high melting points.

Table 1. Analytical and physical data of H_2STH and its complexes. (m.p >300 ^{o}C)

Compound	M.wt.	Color	M.p.; ^{o}C	% Found (Calcd.)					Λ°_m Yield%
				M	Cl	C	H	N	
(H_2STH) $C_{12}H_{12}O_2N_4S$	276.32	White	205	—	—	52.13 (52.16)	4.24 (4.38)	20.78 (20.28)	95
[Co(HSTH)Cl].$2H_2O$ $C_{12}H_{15}ClCoN_4O_4S$	405.73	Dark green	>300	14.78 (14.53)	8.47 (8.74)	35.65 (35.52)	3.74 (3.73)	13.84 (13.81)	88
[Zn(HSTH)Cl(H_2O)] $C_{12}H_{13}ClN_4O_3SZn$	394.17	Pale yellow	>300	16.78 (16.59)	8.56 (8.99)	36.78 (36.57)	3.06 (3.45)	14.89 (14.21)	83

Ion-Flotation Separation of Zn(II):

Flotation-Separation Procedure

A definit concentration of Zn(II) solution, was mixed with a solution of prepared ligand. The pH was adjusted with HNO_3 and/or NaOH. Then, the solution was is completed to 10 mL with bi-distilled water in the flotation cell. To ensure complete complexation, the cell was shacked well for 2 min and then 2 mL of HOL (with definite concentration) were added. Then, the cell was inverted upside down 20 times by hand and left 5 min standing for complete flotation. Finally, the residual concentration of Zn(II) ions was analyzed via AAS. The floatability percentage **F(%) of** Zn(II) ions was calculated according to the following relation:

$$F\ \% = (C_i - C_f) / Ci \times 100 \quad (1)$$

where: C_i and C_f denote the initial and the final concentrations of Zn(II) ions in the mother liquor, respectively.

Biology

Minimum Inhibitory Concentration (MIC)

The synthesized H_2STH and its Co (II) complex tested as anti-bacterial compounds against some strains separated from animal by products and accused of being a main reason for food intoxication in human. Gram-positive bacteria *(Staphylococcus aureus)* and Gram-negative bacteria *(Escherichia coli)* utilized in this experiment using Muller Hinton agar medium (Oxoid). In addition, the anti-fungal properties of these compounds also tested against *(Candida albicans)* using Sabouraud dextrose agar medium (Oxoid).

Ciprofloxacin (100 µg/ml) and Fluconazole (100 µg/ml) were used as standard for anti-bacterial and anti-fungal activity.

Agar streak dilution method used to determine MIC [15] of the compounds. A stock solution of H_2STH and Co(II) complex (100 µg/ml) prepared in DMSO, then definite amounts of the respective compounds were mixed with specific quantity of molten sterile agar (Sabouraud dextrose agar medium for anti-fungal activity and Muller Hinton agar for anti-bacterial activity). A specified quantity of the medium (40—50 °C) containing the compound was poured into a Petri dish to give a depth of 3-4 mm and allowed to solidify. Micro-organism suspension contains about 105 cfu/ml applied to plates with serially diluted compounds dissolved in DMSO and incubated at 37 °C for 24 and 48 h for bacteria and fungi, respectively. The MIC considered as the lowest concentration of the test substances showing an invisible growth of fungi or bacteria on the plate.

Cytotoxicity Assay

Materials and methods

Cell line

Hepatocellular carcinoma (HePG-2), The cell line were obtained from ATCC via Holding company for biological products and vaccines (VACSERA), Cairo, Egypt.

Chemical reagents

The reagents RPMI-1640 medium, MTT, DMSO and 5-fluorouracil (sigma co., St. Louis, USA), Fetal Bovine serum (GIBCO, UK). 5-fluorouracil was used as a standard anticancer drug for comparison.

MTT assay

The cell line was utilized to decide the inhibitory impacts of compounds on cell development utilizing the MTT test [16]. Mitochondrial succinate dehydrogenase was responsible for the colorimetric change of the yellow tetrazolium bromide (MTT) to a purple formazan derivative in suitable cells. The cells were refined in RPMI-1640 medium with fetal bovine serum (10%). Antibiotics (100 units/ml penicillin and 100µg/ml streptomycin) were inserted at 37 ^oC in a 5% CO_2 incubator. The cells were seeded in a 96-well plate at a density of $1.0x10^4$ cells/well under 5% CO_2 at 37 ^oC for 48 h [17]. After a time of incubation, the cells were treated with compounds by different concentration and incubated again for 24 h. After drug treatment (24 h), add 20 µl of MTT solution at 5mg/ml and incubated for 4 h. Add 100 µl dimethyl sulfoxide (DMSO) to each well to dissolve the formed purple formazan. using a plate reader (EXL 800, USA), The colorimetric assay is recorded at an absorbance 570 nm.

$$The\ relative\ cell\ viability\% = \frac{A_{570}\ of\ Treated\ Samples}{A_{570}\ of\ Untreated\ Samples} \times 100$$

Molecular Modeling

DMOL[3] program used to study the cluster calculations [18] in Materials Studio package [19]. Density functional theory DFT semi-core pseudopods calculations (dspp) were done using the double numerical basis sets plus polarization functional (DNP). The DNP basis sets are of comparable quality to 6-31GGaussian basis sets [20]. It was reported previously by Delley et al. that Gaussian basis sets are less accurate than the DNP basis sets of the same size [21]. The RPBE functional is employed to take account of the exchange and correlation effects of electrons , where it is so far considered the best exchange–correlation functional [22] based on the generalized gradient approximation (GGA) [23]. The geometric optimization displayed without any symmetry limitation.

Results and Discussion

IR Spectra of H_2STH and Complexes.

Table (2) show the most important assignments of IR spectral bands (in KBr) of H_2STH and its complexes. In order to assign the characteristic bands of the coordinates sites of H_2STH (structure 1) to the metal ions. The IR spectrum bands of the free H_2STH shows five bands at 1670, 1610, 1531, 3339 and 3128 cm^{-1} attributed to ν(C=O), $\nu(C=N)_{ring}$, $\nu(C=N)_{az}$, $\nu(OH)_{phenolic}$ and $\nu(NH)_{sym}$, respectively. The ν(N-N) at 986 cm^{-1} and ν($-NH_2$→=NH) of the ring at 3301 cm^{-1} shifted to higher frequencies upon complexation [24, 25] .

Table 2. Assignments of IR spectral bands of H_2STH and its complexes.

Compound	ν(C=O)	$\nu(C=N)_{az}$	$\nu(C=N)_{ring}$	$\nu(NH_2)$	$\nu(NH)_{sym}$	υ(C=N)*	υ(C-O)	ν(N-N)	ν(OH)	ν(M-O)	ν(M-N)
H_2STH	1670	1531	1610	3301	3128	-	1265	986	3339	-	-
$[Co(HSTH)Cl].2H_2O$	-	1549	1608	3365	-	1512	1242	1043	3382	547	469
$[Zn(HSTH)Cl(H_2O)]$	-	1553	1622	3384	-	1522	1250	1044	3433	542	467

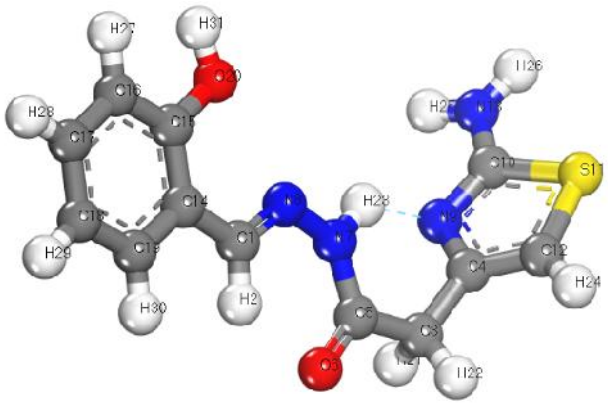

Structure 1.Molecular modeling of H_2STH

H_2STH coordinates as mononegative tridentate via $(C=N)_{az}$, $(C=N)_{ring}$ and enolized (CO) with deprotonation in Co(II) complex (structure 2). Also, H_2STH behaves as mononegative bidentate in Zn(II) complex (structure 3) coordinating via $(C=N)_{az}$ and (CO) enolized with deprotonation. both behaviors are suggested by the following evidences:

i. The shift of $\nu(C=N)_{az}$ to lower wavenumber and the shift of ν(N-N) to higher wavenumber.[26, 27].

ii. The disappearance of both ν(CO) and ν(NH) with simultaneous appearance of new bands assigned to ν(C-O) and $\nu(C=N)^*$.

iii. The shift of $\nu(C=N)_{az}$ and $\nu(C=N)_{ring}$ to lower wavenumbers in Co(II) complex.

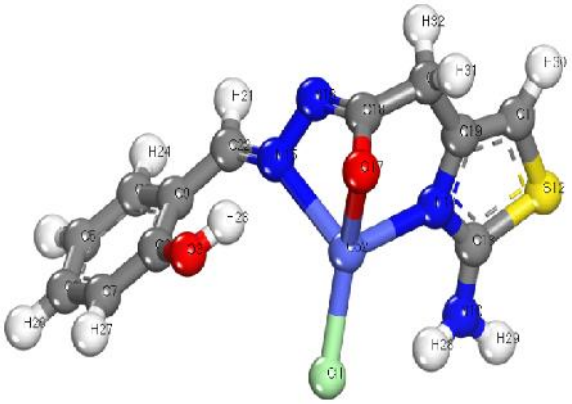

Structure 2.Molecular modeling of [Co(HSTH)Cl].2H_2O

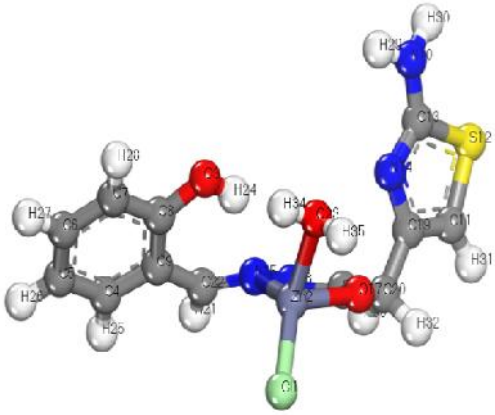

Structure 3.Molecular modeling of [Zn(HSTH)Cl(H_2O)]

^{1}H and ^{13}C-NMR Spectra of the H_2STH

.

The ^{1}NMR spectrum of H_2STH (fig. 1) in d_6-DMSO shows two signals at δ=11.16 and 11.73 ppm relative to TMS which disappear after addition D2O (fig. 2) and can be attributed to NH and OH protons, respectively. The doublet protons signal at 3.41 ppm and signal proton at 3.78 ppm assigned to CH_2 and CH protons, respectively. The multiplets at 6.27-7.61 ppm are due to the phenyl and CH of thiazole ring protons. The signals 8.26-8.40 ppm may be assigned to -NH_2 and =NH protons of thiazole ring.

In the ^{13}C-NMR spectrum (fig. 3), the carbon resonance signals of the CO, $CN_{(azomethine)}$ and $CN_{(ring)}$ groups appeared at δ= 170.75, 168.25 and 165.32 ppm, respectively. The signal of C-OH $_{phenolic}$ appear at 157.29 ppm. Moreover, the signals at 146.90, 145.07 and 141.03 ppm assigned to both C-S and C-N of ring moiety and C-N of open chain hydrazide group.

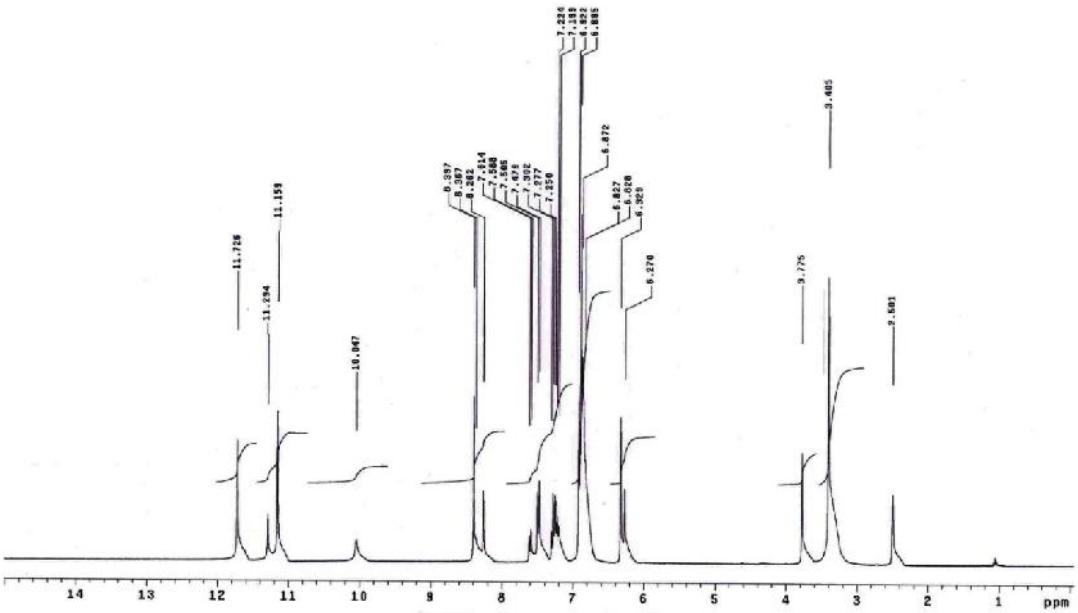

Figure 1: ^{1}HNMR spectra of H_2STH in d_6-DMSO.

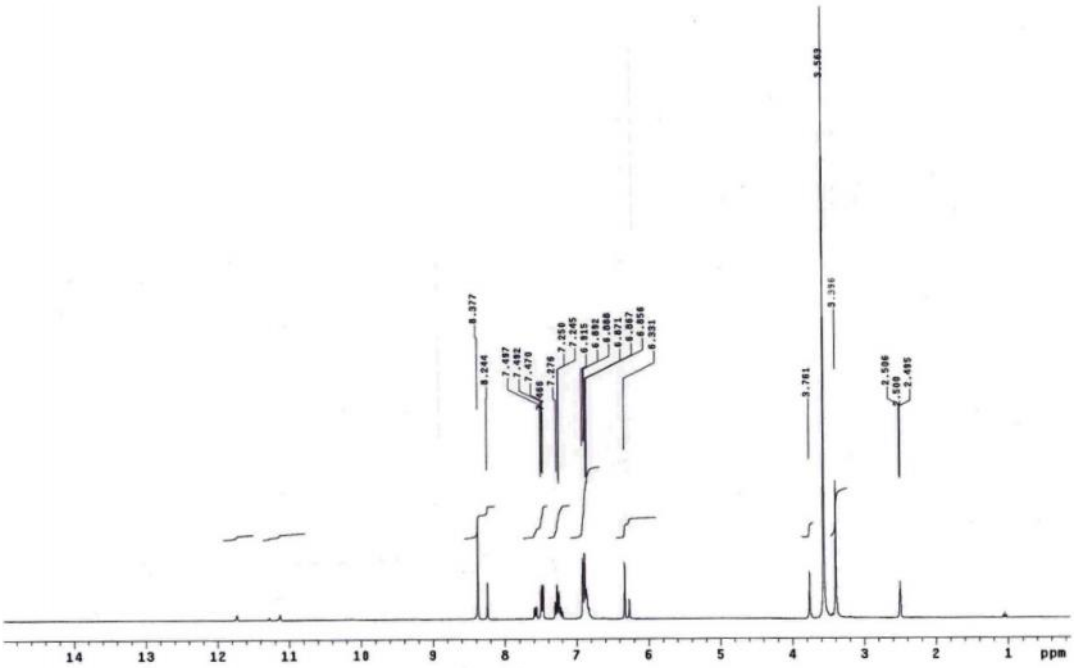

Figure 2: ^{1}HNMR spectra of H_2STH in d_6-DMSO with addition of D_2O

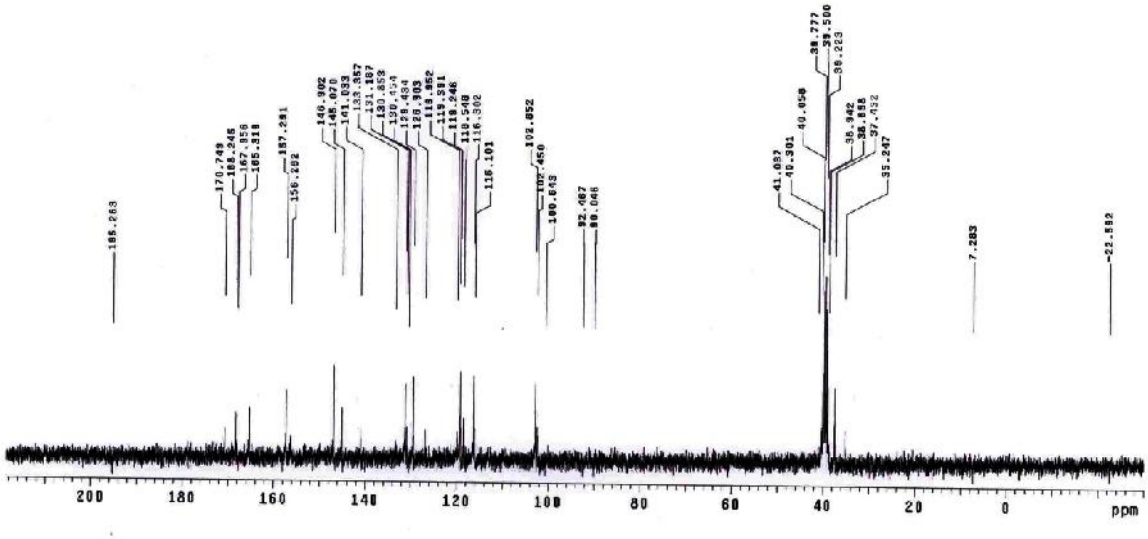

Figure 3: ^{13}CNMR spectra of H_2STH d_6-DMSO.

Magnetic properties and electronic spectra:

The assignments of the spectral bands for H_2STH and its complexes in DMSO and the magnetic moments are compiled (table 3). The H_2STH showed two absorption bands at 35714 and 32258 cm^{-1} assigned to π-π^* and one strong band at 29412 cm^{-1} attributed to n-π^* of both C=O and C=N groups. [28, 29].

The deep green colour, the magnetic moment value and spectral bands of the Co(II) complex are more consistent with tetrahedral geometrical structure. The $[Co(HSTH)Cl].2H_2O$ spectrum show a bands at 20921 and 24631 cm^{-1} assigned to $^4A_2(F) \rightarrow {}^4T_1(P)(\nu_3)$. In the chloride complex the shoulder at 14743 cm^{-1} due to spin-orbit coupling indicating a tetrahedral geometry for the complex.

Table 3: Electronic spectral data of H_2STH and its complexes.

Compound	Band position,cm^{-1}	μ_{eff}(B.M)
H_2STH	35714, 32258, 29412	-
$[Co(HSTH)Cl].2H_2O$	35971, 32258, 29070, 24631, 14743	4.48

Thermogravimetric Studies.

The TG and DTA for the respective complexes are depicted in Figs. (4 and 5). The obtained data approved the proposed formulae. Where, it is clear that the represented steps of complex degradation is three. The first in which the crystalline water is removed at 36–74 ^oC and then the coordinated water at 170–373 ^oC. Then, the degradation process began 250–800 ^oC and at the end, formation of metal oxide took place.

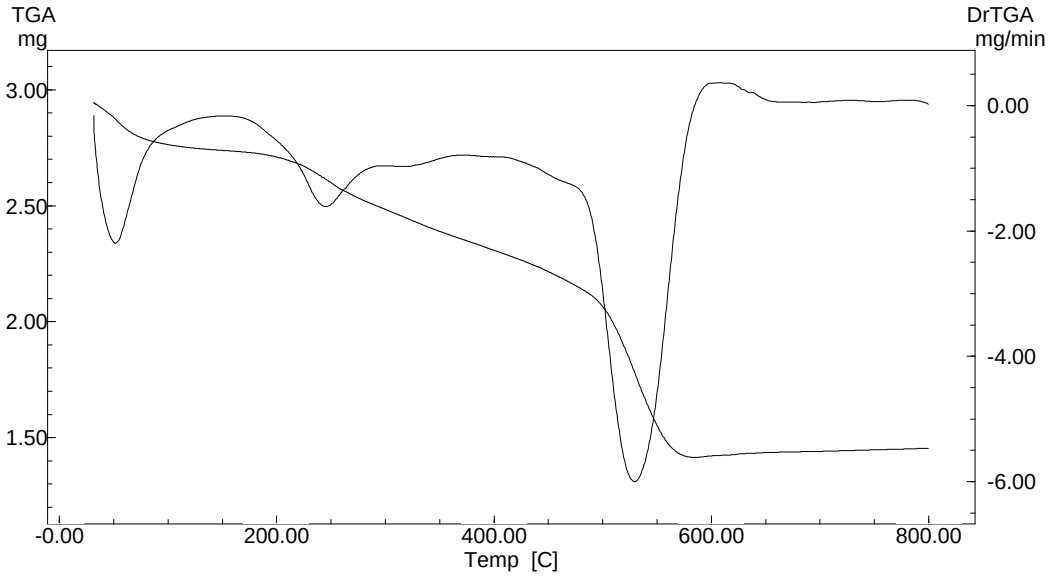

Figure 4: Thermal analysis curves (TGA, DTG) of $[Co(HSTH)Cl].2H_2O$ Complex.

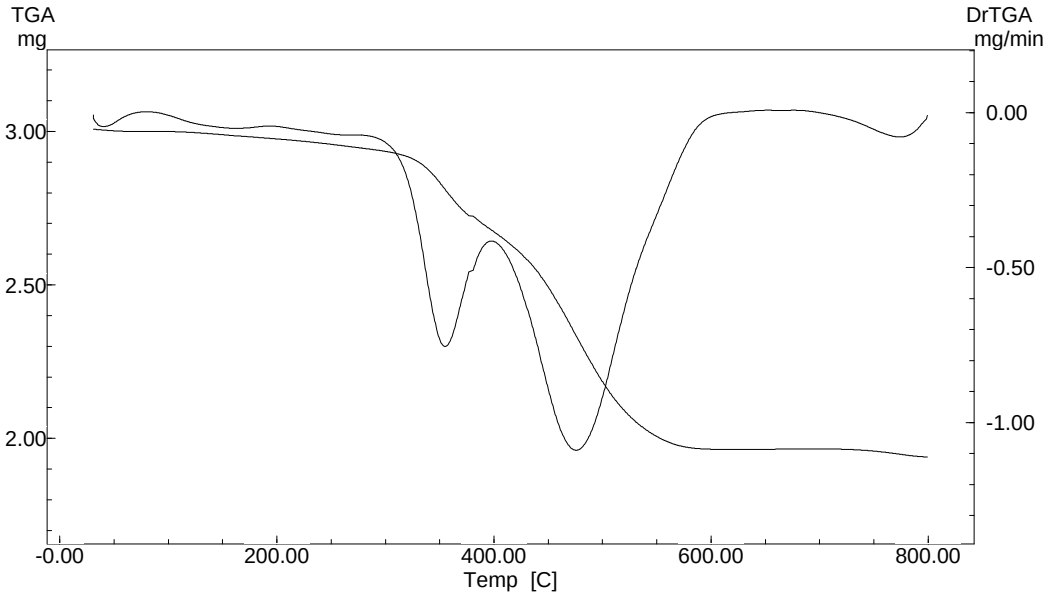

Figure 5: Thermal analysis curves (TGA, DTG) of $[Zn(HSTH)Cl(H_2O)]$ Complex

Kinetic Data of Thermal Degradation:

The kinetic parameters of decomposition stages have been evaluated by using non-isothermal methods. The rate of degradation, dα/dt, is a linear function of rate constant k (temperature dependent) and function of conversion α (temperature independent) and can be expressed as follow [a]:

$$d\alpha/dt = K(T)f(\alpha) \qquad (2)$$

The reaction rate constant, k, has been calculated by the Arrhenius expression:

$$K = Ae^{-E/RT} \qquad (3)$$

Where R is the gas constant, E is the activation energy and A is the pre-exponential factor. Substituting Eq. (3) into Eq. (2), we get:

$$d\alpha/dt = A\left(e^{-\frac{E}{RT}}\right)f(\alpha) \qquad (4)$$

When the temperature varied by a constant and controlled heating rate, Φ=dT/dt, the change in degree of conversion which is a function of temperature dependent also on time of heating. Therefore Eq. (4) becomes:

$$d\alpha/dt = A/\emptyset\left(e^{-\frac{E}{RT}}\right)f(\alpha) \qquad (5)$$

The integrated form of Eq. (5) is generally expressed as:

$$g(\alpha) = \int_0^{\alpha}\frac{d\alpha}{f(\alpha)} = A/\emptyset\int_0^{T} e^{-E/RT}\,dt \qquad (6)$$

where $g(\alpha)$ is the integrated form of the conversion dependence function. The right-hand side integral of Eq. (6) is known as temperature integral and has no closed form solution. The most used methods for evaluation of temperature integral are method of Coats-Redfern Figs. 6 and 7 [30] and the approximation method of Horowitz-Metzger Figs. 8 and 9 [31]. From the results obtained, the following remarks can be pointed out:

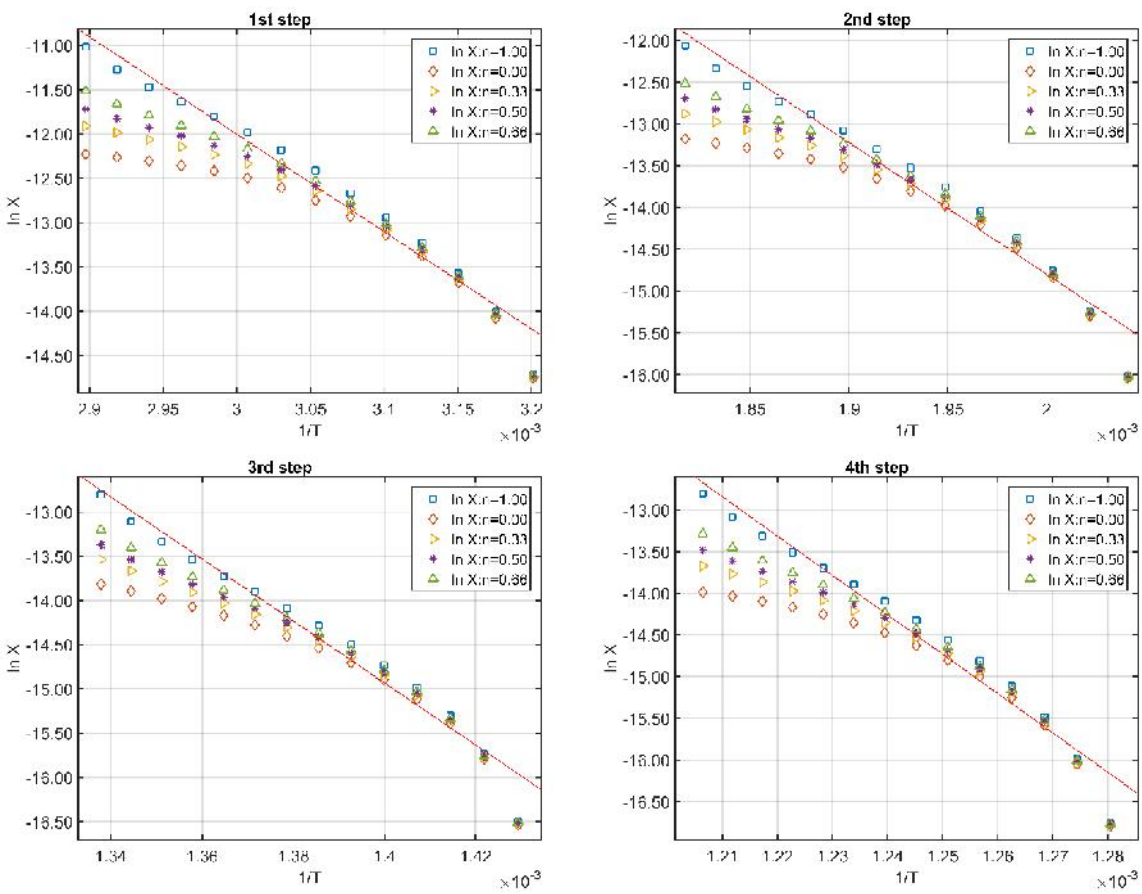

Figure 6: Coats-Redfern plots of [Co(HSTH)Cl].2H_2O

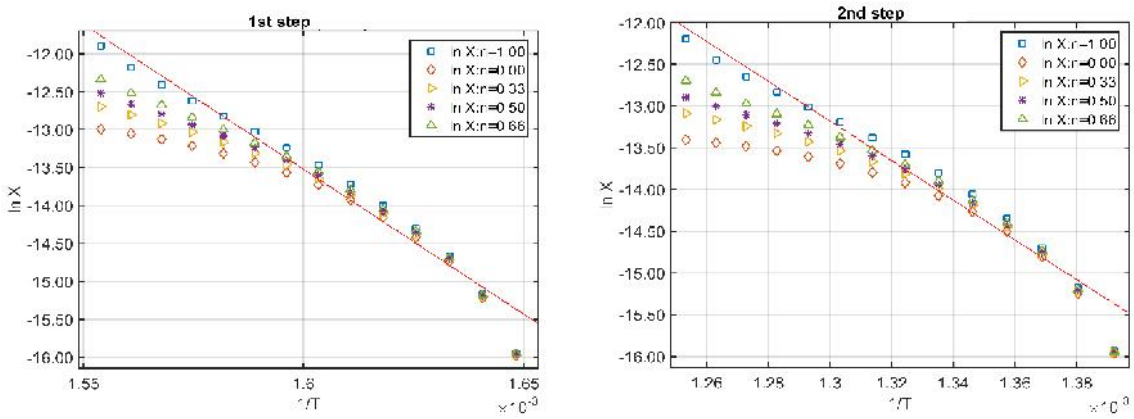

Figure 7: Coats-Redfern plots of [Zn(HSTH)Cl(H_2O)]

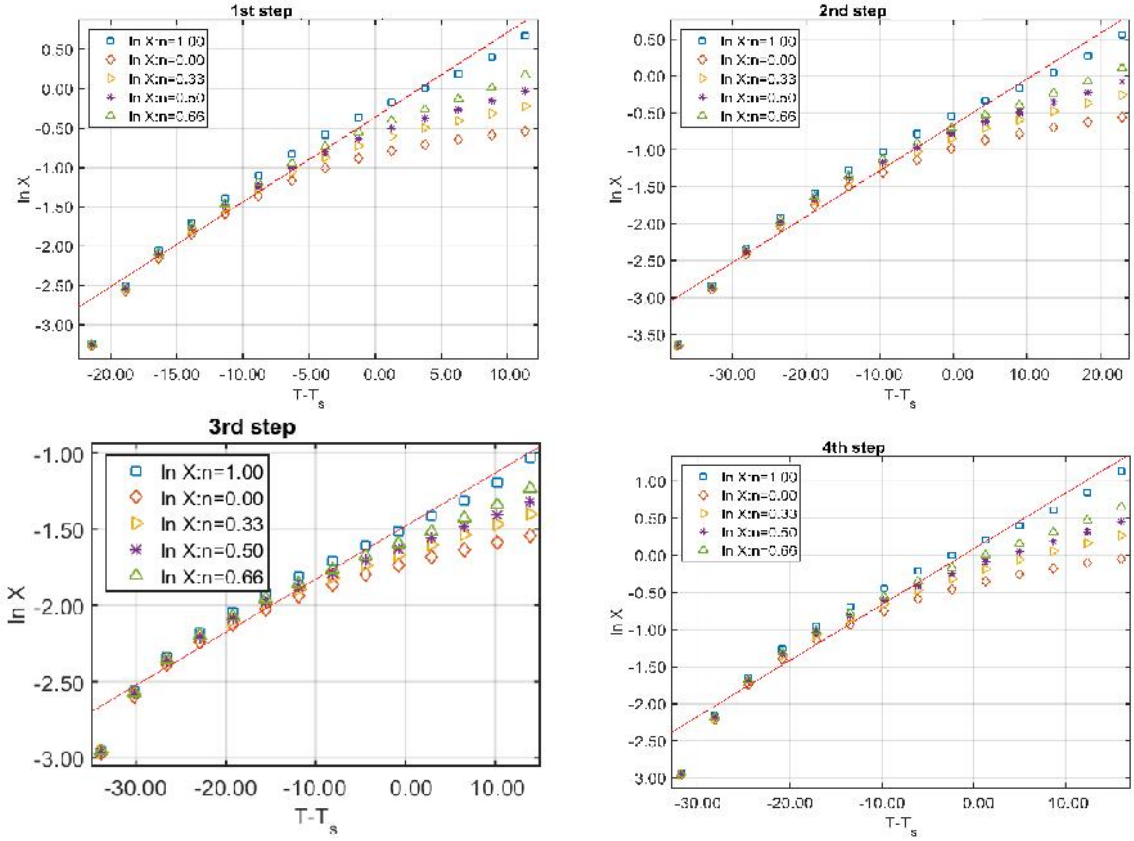

Figure 8: Horowitz- Metzger plots of [Co(HSTH)Cl].2H_2O

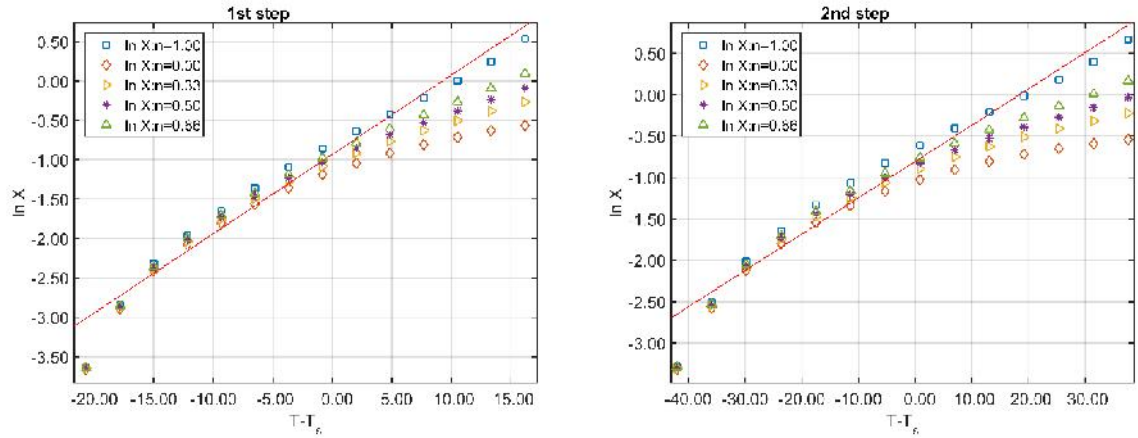

Figure 9: Horowitz- Metzger plots of [Zn(HSTH)Cl(H_2O)]

(i) The kinetic parameters (E, A, ΔH, ΔS and ΔG) of all prepared solid complexes have been calculated by CR and HM method (Table 4). The values of parameters from the two methods are quite comparable.

(ii) at (n=1) (first order degradation), all steps show a best fit in all cases. Other n values (eq.4 and 5) did not satisfy to good correlations.

(iii) The exceed of ΔG value because the value of TΔS significantly from one stage to another which overrides the value of ΔH. Increasing the value of ΔG of a given complex on going from one decomposition step to another displayed that the rate of H_2STH removal will be lower from step to the subsequent step [32, 33]. This behavior due to the high structure rigidity of remaining complex after the explosion of one or more H_2STH for remaining complex.

(iv) The values of the entropy of activation, ΔS* of the decomposition steps of the metal complexes indicate that the activated fragments have more ordered (negative values) or disordered (positive values) structure than the undecomposed complexes and/or the slowing of decay reaction[30].

(v) The positive value of ΔH means the endothermic nature of the decomposition processes.

Table 4. Kinetic Parameters evaluated by Coats-Redfern and Horowitz-Metzger equations for the prepared complexes.

Compound	step	Mid Temp.(K)	Method	E_a KJ\mol	A (S^{-1})	ΔH* KJ\mol	ΔS* KJ\mol.K	ΔG* KJ\mol
[Co(HSTH)Cl].2H_2O	1st	328.79	HM	96.63	2.70×10^{13}	93.90	0.0114	90.14
			CR	91.37	4.11×10^{12}	88.64	-0.0042	90.04
	2nd	517.35	HM	138.08	4.14×10^{11}	133.78	-0.0271	147.80
			CR	131.29	9.04×10^{10}	126.99	-0.0397	147.55
	3rd	723.55	HM	302.89	4.43×10^{19}	296.88	0.1238	207.28
			CR	291.36	6.67×10^{18}	285.34	0.1081	207.13
	4th	802.85	HM	403.14	1.10×10^{24}	396.47	0.2071	230.21
			CR	392.63	2.34×10^{23}	385.95	0.1942	230.03
[Zn(HSTH)Cl(H_2O)]	1st	622.36	HM	324.37	1.11×10^{25}	319.20	0.2284	177.02
			CR	317.42	2.99×10^{24}	312.25	0.2175	176.86
	2nd	750.35	HM	205.41	6.93×10^{11}	199.17	-0.0259	218.60
			CR	197.63	2.11×10^{11}	191.39	-0.0358	218.25

Generally, the value of stepwise stability constants decreases with an increase in the number of atoms of H_2STH attached to the metal ion [34, 35] therefore a reverse effect may occur during the decomposition process. Hence the rate of removal of the remaining H_2STH will be lower than that of the rate before the explosion of H_2STH.

Molecular Modeling.

The atom numbering in the structure of H_2STH molecule and its complexes are depicted in Structures (1- 3). From the analysis of the data calculated for the bond lengths and angles, one can conclude the following:

i. The bond angles of the hydrazone moiety of H_2STH were changed slightly upon coordination; the largest change affects in H_2STH are C(10)-N(9)-C(4), N(7)-C(5)-O(6), N(7)-N(8)-C(1), N(8)-N(7)-C(5) and O(20)-C(15)-C(14) angles. The bond angles in ligand may be varied to lower or higher values on complexation as a consequence of bonding [36].

ii. The bond angles in metal complexes afforded a tetrahedral geometry with sp^3 hybridization [30].

iii. All the active groups in taking part in coordination have bonds longer than that already exist in the ligand moiety like $(C\text{-}O)_{enol}$, $C{=}N_{azomethine}$ and $C{=}N_{ring}$ This is referred to the formation of the M-N bond which makes the C-N bond weaker as a result of coordination via N atom of (C=N) [37]

iv. The bond lengths of C(1)-N(8) and C(5)-N(7) become slightly weaker and longer in complexes because the withdrawing of electrons density as a result of coordination via N atoms of -C=N-C=N- group that is formed enolization followed by deprotonation of OH group in all complexes [36].

v. The bond distance of $(CO)_{enolic}$ that participate in coordination becomes weaker and longer as a result of the M-O bond formation[38]

vi. The bond angles of ligand side containing atoms of coordination will be changed in both complexes because the N-M-O formation ring [39].

The energies of both HOMO (π donor) and LUMO (π acceptor) are main parameters in quantum chemical studies. Where, HOMO is the orbital that acts as an electron donor, LUMO is the orbital that act as the electron acceptor and these molecular orbitals are known as the frontier molecular orbitals (FMOs) Fig. 10.

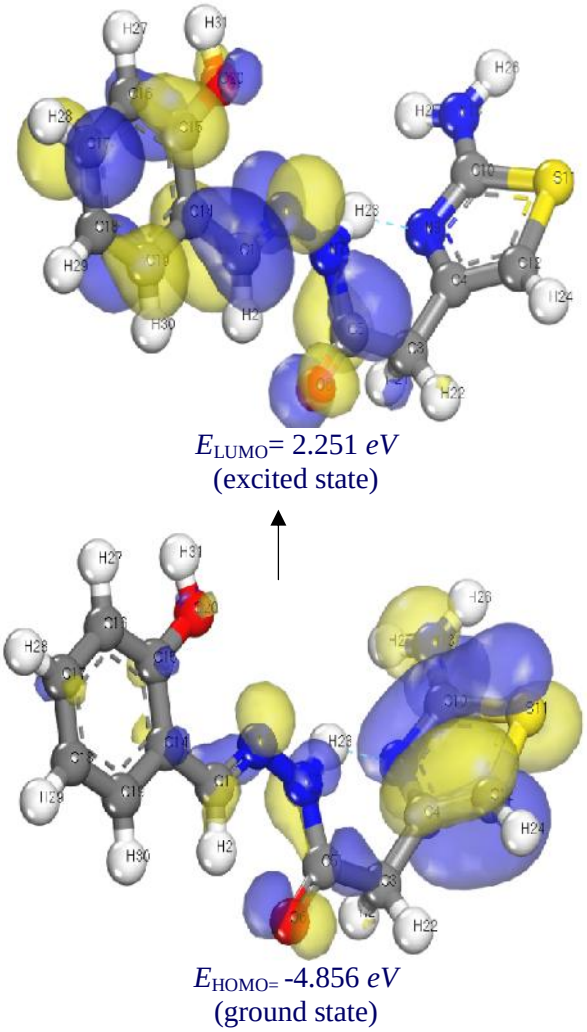

Fig 10. 3D plots frontier orbital energies using DFT method for H_2STH.

In many reactions, the overlap between HOMO and LUMO orbitals considered as a governing factor, where in H_2STH; the orbitals with the higher molecular orbital coefficients can be considered as the main sites of coordination. The energy gap (E_{HOMO} - E_{LUMO}) is a significant stability index facilitate the characterization of both kinetic stability and chemical reactivity of the molecules [40]. Molecules with a small gap are known as soft molecules, they are more polarized and more reactive than hard ones because they easily offer electrons to an acceptor. In H_2STH, the energy gap is small showing that charge transfers easily in it and this influences the biological activity of the molecule. Moreover, the low value of energy gap is due to the groups that enter into conjugation [41].

DFT method sites the selectivity of the molecular systems and concepts the chemical reactivity. The energies of frontier molecular orbitals (E_{HOMO}, E_{LUMO}), electronegativity (χ), energy band gap which explains the eventual charge transfer interaction within the molecule, global hardness (η), chemical potential (μ), global electrophilicity index (ω) and global softness (S) [42, 43] are listed in Table 5.

$\chi = -1/2\ (E_{LUMO} + E_{HOMO})$ (7)
$\mu = -\chi = 1/2\ (E_{LUMO} + E_{HOMO})$ (8)
$\eta = 1/2\ (E_{LUMO} - E_{HOMO})$ (9)
$S = 1/2\ \eta$ (10)
$\omega = \mu^2/2\ \eta$ (11)
The softness (σ) is the inverse number of (η) as follow:
$\sigma = 1/\eta$ (12)

Table 5. Calculated E_{HOMO}, E_{LUMO}, energy band gap ($E_H - E_L$), chemical potential (μ), electronegativity (χ), global hardness (η), global softness (S) and global electrophilicity index (ω) for H_2STH and its complexes.

Compound	E_H (eV)	E_L (eV)	(E_H - E_L) (eV)	χ (eV)	μ(eV)	η (eV)	S (eV^{-1})	ω(eV)	σ (eV)
H_2STH	-4.856	-2.251	-2.605	3.554	-3.554	1.303	0.651	4.847	0.768
[Co(HSTH)Cl].2H_2O	-4.107	-2.455	-1.652	3.281	-3.281	0.826	0.413	6.516	1.211
[Zn(HSTH)Cl(H_2O)]	-4.563	-2.468	-2.095	3.516	-3.516	1.048	0.524	5.899	0.955

Ion-Flotation Separation of Zn(II):

Effect of initial pH

Numerous experiments were carried out to study the effect of initial pH on the floatability of 2×10^{-4} mol.L^{-1} of metal ions using 2×10^{-4} mol.L^{-1} of prepared ligand and 1×10^{-3} mol.L^{-1} of HOL. The results attained are presented in figure 11. It can be seen that, highest floatability were reached at the pH range (6-10) for Zn^{2+} ions. This facilitates the application of the prepared ligand for the separation of metal ions from different media.

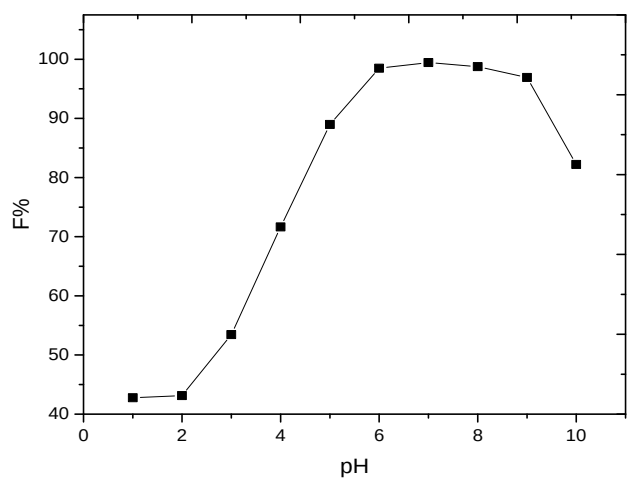

Fig. 11: Influence of pH on the floatability of 2×10^{-4} mol L^{-1} Zn^{2+} ions using 2×10^{-4} mol and 1×10^{-3} mol.L^{-1} HOL.

Effect of initial metal concentration

Tries to float variable concentrations of Zn^{2+} ions using 2×10^{-4} mol.L^{-1} of prepared ligand and 1×10^{-3} mol.L^{-1} HOL at pH~7 were carried out. The deduced data in figure 12 indicated that the high flotation efficiency (~100%) of Zn^{2+} ions was obtained and remains constant for the prepared ligand whenever the ratio of M:L is (1:1). The chelating agent gave quantitative separation of Zn^{2+} ions (~100%) which may be due to the presence of enough amounts of prepared ligand to bind all Zn^{2+} ions.

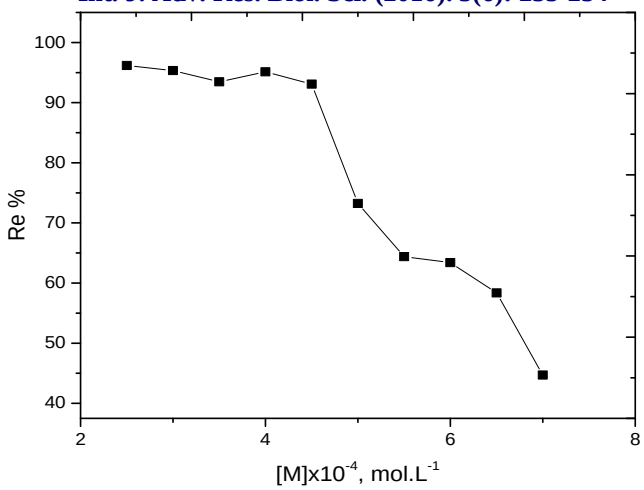

Fig. 12: Floatability of several concentrations of Zn^{2+} ions using 2×10^{-4} mol L^{-1} of prepared ligand and 1×10^{-3} mol L^{-1} HOL at pH ~7.

Effect of ligand concentration

The collecting ability of prepared ligand towards Zn^{2+} ions was tested using 1×10^{-3} mol.L^{-1} HOL at pH~7. The data presented in figure 13 show that, the floatability of Zn^{2+} ions exceeds sharply reaching its highest value (~100%) at M:L ratio of (1:1). The addition of more ligand has no adverse effect on the flotation process, accordingly 2×10^{-4} mol.L^{-1} of prepared ligand was used throughout.

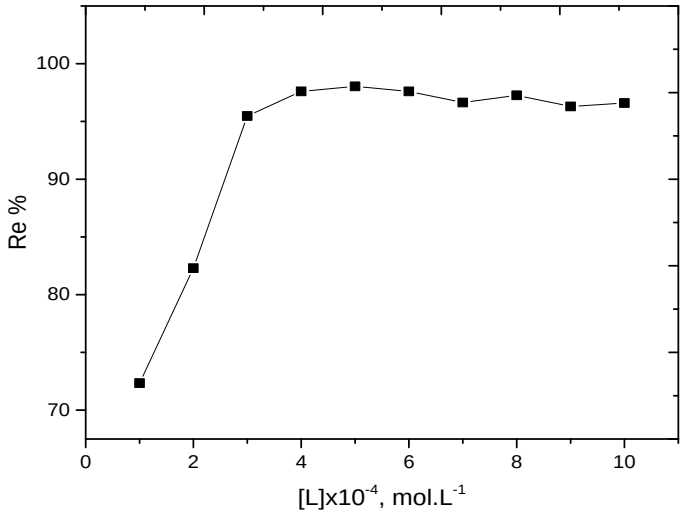

Fig. 13: Floatability of 2×10^{-4} mol L^{-1} Zn^{2+} ions using different concentrations of prepared ligand and 1×10^{-3} mol L^{-1} HOL at pH ~7.

Effect of surfactant concentration

Trials were performed to float Zn^{2+} ions with HOL only, but the efficiency of recovery does not outdo 27.5 %. Therefore, another series of experiments were performed to float 2×10^{-4} mol.L^{-1} Zn^{2+} ions in the presence of 2×10^{-4} mol.L^{-1} of prepared ligand and different concentrations of HOL (1×10^{-3}-5×10^{-2} mol.L^{-1}) at pH~7. The outcomes obtained in figure 14 show that in HOL at concentration range of 1×10^{-3}-9×10^{-3} mol.L^{-1}, high floatation % of Zn^{2+} is achieved.

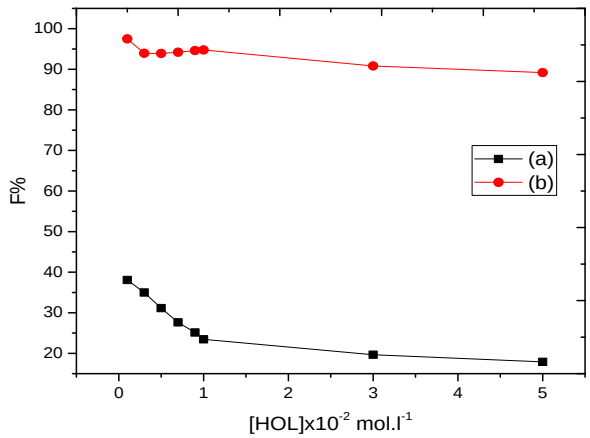

Fig. 14: Floatability of 2×10^{-4} mol L^{-1} Zn^{2+} ions with (a) and without (b) of 2×10^{-4} mol L^{-1} of prepared ligand at pH ~7 using different concentrations of HOL.

At oversize surfactant amount the incomplete extraction of Zn^{2+} ions may be lead to the surfactant changes the state of the particles, Zn^{2+}-ligand precipitates, from coagulation precipitation through coagulation flotation to re-dispersion with an increase in the amount of HOL added [44]. Also, at high surfactant concentration poor flotation is produced due to the formation a stable, hydrated envelope of surfactant on the air bubble surface or, by forming a hydrate micelle coating on the solid surface .[45, 46].

Effect of temperature

A solution containing Zn^{2+} ions and the prepared ligand and another solution containing HOL were either heated in a water bath or cooled in an ice bath to the same temperature. The HOL solution was quickly poured into Zn^{2+} ions solution. The mixture was introduced into the flotation cell. The flotation procedure was then followed. The obtained results in figure 5 showed that maximum flotation (~100%) of Zn^{2+} ions in the range 15-80˚C. The decrease in separation when the temperature overtop 80˚C may be due to the excess in solubility of the precipitate, the instability of the foam causative partial dissolution of the precipitate and insufficient foam consistency to hold up the precipitate [47].

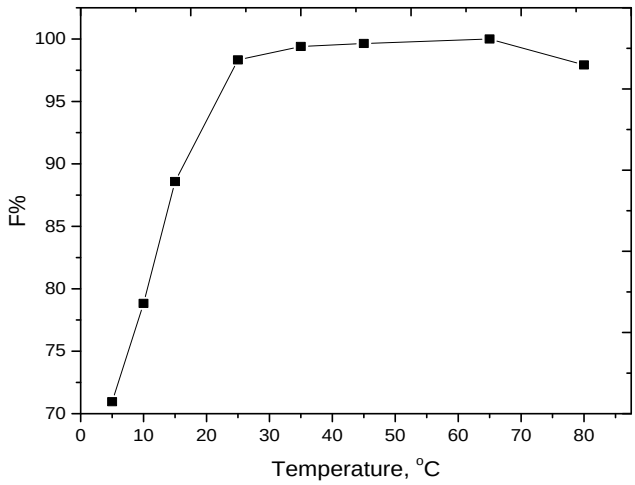

Fig. 15: Floatability of 2×10^{-4} mol L^{-1} Zn^{2+} ions at different temperatures using 2×10^{-4} mol L^{-1} of prepared ligand and 1×10^{-3} mol L^{-1} HOL at pH ~7.

Effect of presence of foreign ions

Under the ideal conditions determined for this investigation, the percentage removal of Zn^{2+} ions from a solution of pH 7 containing 30 $mg.L^{-1}$ of prepared ligand was studied in the presence of high concentrations of various cations and anions. All the chloride salts of cations and the sodium or potassium salts anions were used. The acceptable amounts of each ion, giving an error of ± 4% in the removal efficiency of Zn^{2+} ions are listed in table 6. Inspection of the data indicates that, all the investigated foreign ions with relatively high concentrations have no adverse effect on the flotation of zinc.

Table 6 Effects of the foreign ions on the removal percentage of the examined metal ions: [M = 2×10^{-4} $mol.L^{-1}$; Ligand = 2×10^{-4} $mol.L^{-1}$; HOL = 1×10^{-3} $mol.L^{-1}$; pH = 7]:

Ion	Interference/analyte ratio ($mg\ L^{-1}$)	Re, %
Na^+	25	99.1
K^+	20	96.2
Mg^{2+}	25	100
Ca^{2+}	30	97.1
Cl^-	15	97.2
SO_4^{2-}	35	95.9
HCO_3^-	25	96.9
CH_3COO^-	35	97.4

Application

To investigate the applicability of the recommended procedure, a multi tries were performed to recover Zn^{2+} ions spiked to 1L of aqueous samples. The flotation experiments were carried out using 50 mL filtered sample solutions at pH 7. The deduced data presented in table 7 show that the recovery was quiet and quantitative under the recommended conditions of the applied flotation procedure.

Table 7: Recovery of studied metal ions spiked to several water samples: [Ligand = 2×10^{-4} $mol.L^{-1}$; HOL = 1×10^{-3} $mol.L^{-1}$; pH ~7]

Water samples (location)	Zn^{2+}	
	Added metal ($mg.L^{-1}$)	Re %
Sharm El-Shiekh	3.8	95.97
Alexandria	3.8	96.71
New Valley	3.8	93.26
Mansoura	3.8	95.34

Ion-flotation mechanism

The flotation stages of analyte-ligand precipitates is suggested depending on the following points:

1. Zn^{2+} coordinate with the prepared ligand in a M:L ratio of (1:1) to give the complex M_2L according to the following equation:

$$M^{2+} + H_2L = M_2L + 2H^+$$

The prepared ligand has many centers containing atoms of high electron density, such as O and N in the form of C=O, NH and C=N, functional groups as shown in table 2, capable of forming hydrogen bonds.

1. Oleic acid begins to dissociate at pH > 5.2 [48] and the percentage of different forms of oleic acid are determined by IR analysis and the data is presented in table 8 (Pol'kin et al., 1968). The IR spectra of oleic acid with changing pH indicated that at 1300-1800 cm^{-1}, there are bands characteristic of the groups COOH, COO^- and COO^- contained with Na [49]. These data agree with those reported [50] that the C=O stretching band of oleic acid at 1705 cm^{-1} is shifted on ionization to bands in the range 1520 -1540 cm^{-1} for sodium oleate. Therefore, oleic acid can

2. inserted with other systems, across hydrogen bonding, either in its molecular (R-COOH) or dissociated ($R\text{-}COO^-$) forms depending on the pH of the enviroments and according to the following:

$$R\text{-}COOH + M_2L = R\text{-}COOH\ldots. LM_2$$

$$R\text{-}COO^- + M_2L = R\text{-}COO^-\ldots. LM_2$$

3. The insertion of oleic surfactant with both copper and zinc chelates gives hydrophobic aggregates that float with the aid of air bubbles to the surface of the solution [51].

Table 8: Different forms of oleic acid determined by spectrophotometric study [50]

pH	(%)			Total
	HOL	Ol^-	NaOL	
5.2	100.0	0.0	0.0	100.0
8.0	6.5	34.2	0.0	100.0
8.2	38.5	57.7	3.8	100.0
9.0	13.6	68.2	18.2	100.0
11.5	0.0	80.0	20.0	100.0
12.0	0.0	52.2	47.8	100.0

Conclusion

This investigation presents (ligand name) derivative as organic chelate for the separation of about 100% of Zn^{2+} ions. This quality and perfect outcomes satisfied by using the simple, rapid and inexpensive flotation technique. Now, this technique is applicable soon incorporated as a clean technology to treat water and wastewater. The procedure is free from interferences, does not affected by raising temperature up to 65˚C (which giving a chance for application to hot wastewater without need for cooling) making the process economic. It is also successfully applied to the recovery of Zn^{2+} ions spiked into different environmental water samples. The formation of hydrogen bonding between surfactant and zinc complex is the backbone step in the flotation mechanism.

Biological Activity

Minimum Inhibitory Concentration (MIC)

H_2STH and its Co(II) complex were tested for their antibacterial potency against *Staphylococcus aureus* (*S. aureus*) as an example of Gram-positive bacteria, *Escherichia coli (E. coli)* as examples of Gram-negative bacteria and against a pathogenic *Candida albicans (C. albicans)* fungal strain. The Activities of Antimicrobial and Antimycotic Activities in terms of MIC (µg/mL) in Table 9. The fungicide Fluconazole and the bactericide Ciprofloxacin were used as references to compare the potency of the respective compounds under one conditions.

Table 9. Antimicrobial and Antimycotic Activities in terms of MIC (µg/mL).

Compound	***E. coli***	***S. aureus***	***C. Albicans***
H_2STH	6.25	1.56	3.12
$[Co(HSTH)Cl].2H_2O$	2.34	0.78	1.56
Ciprofloxacin	1.56	0.78	----
Fluconazole	----	----	1.17

$[Co(HSTH)Cl].2H_2O$ is the most potent followed by the ligand when compared with reference compounds with MIC (2.34 and 6.25 µg/mL), (0.78 and 1.56 µg/mL) and (1.56 and 3.12 µg/mL) for *E.coli, S. aureus* and *C. albicans*, respectively.

Cytotoxicity Assay

In our experiments, IC_{50} values (compound concentration that produces 50% of cell death) in micro molar units were calculated. For comparative aims the cytotoxicity of Fluorouracil (5-FU) the free ligand and its complexes has been studied under one conditions.

It is found that chelation with metal has no synergistic effect on the cytotoxicity. Importantly, it should be emphasized that [Co(HSTH)Cl].2H_2O complex show strong activity nearly to that of Fluorouracil (8.80 µmol/L) for (HePG-2). These gratifying results are encouraging its further screening in vitro. Later on, upon further analysis, this ligand also exhibits considerable cell growth inhibition activity against human liver hepatocellular carcinoma (HePG-2) cells. thereby, its further biological evaluation in vivo as well as studies of mechanism of action is important [11].

As shown in table 10, the tested human tumor cells of hepatocellular carcinoma (HePG-2) Figure 16, Show greater response with [Co(HSTH)Cl].2H_2O complex with IC_{50}=8.8 µmol/L. while, the ligand show strong results of IC_{50} (µmol/L) = 12.2 against (HePG-2).

Table 10. In vitro Cytotoxicity IC_{50} activity of H_2STH and its Co(II) complex against human tumor cells hepatocellular carcinoma (HePG-2)

Compound	In vitro Cytotoxicity IC_{50} (µmol/L)
	HePG-2
5-Fluorouracil	7.9±0.84
H_2STH	12.2±1.23
[Co(HSTH)Cl].2H_2O	8.8±0.98

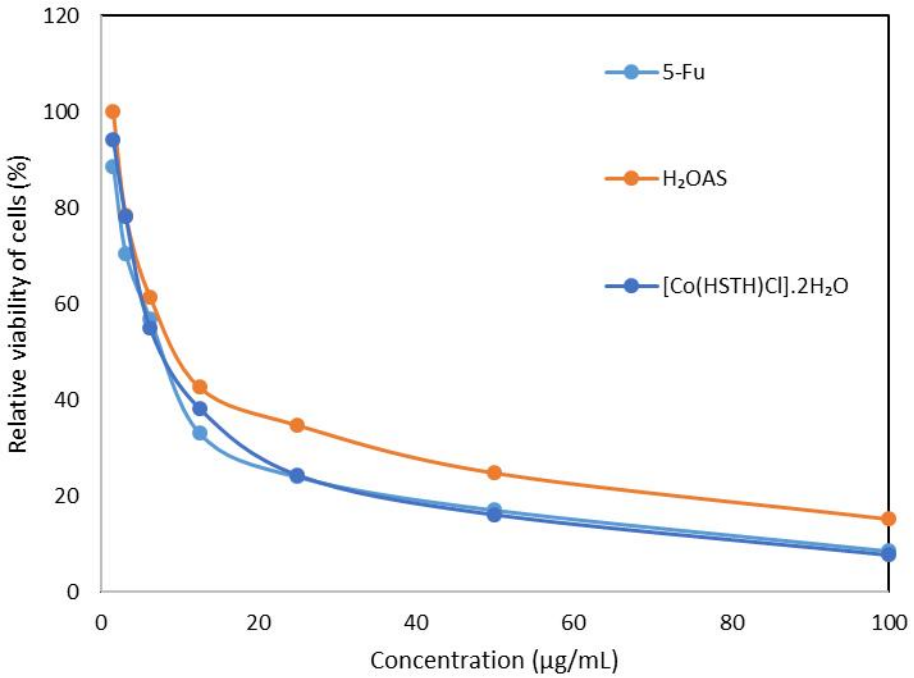

Fig. 16. Relative viability of tumor cells with concentration of H_2STH and its Co(II) complex

Conclusion

The thiazol hydrazone derived from the condensation 2-(2-aminothiazol-4-yl)acetohydrazide with 2-hydroxy benzaldehyde (salicylaldehyde) and its Co(II) and Zn(II) chelates were synthesized. The data of IR spectra indicate that the H_2STH coordinates as mononegative tridentate via $(C=N)_{az}$, $(C=N)_{ring}$ and enolized (CO) with deprotonation in Co(II) complex. Also, H_2STH behaves as mononegative bidentate in Zn(II) complex coordinating via $(C=N)_{az}$ and (CO) enolized with deprotonation. The proposed geometries of isolated complexes were proved using DFT. The ion-flotation the hydrazone derivative as organic chelate for the separation of about 100% of Zn^{2+} ions procedure is free from interferences, does not affected by raising temperature up to 65˚C (which giving a chance for application to hot wastewater without need for cooling) making the process economic. Co(II) complex shows the highest Cytotoxicity activity and minimum inhibitory concentration (MIC) activity against *Staphylococcus aureus*, *Escherichia coli* and *Candida albicans.*

References

[1] Blanz, E. J., and French, F. A. 1968. The carcinostatic activity of 5-hydroxy-2-formylpyridine thiosemicarbazone, *Cancer Res. 28*, 2419-2422.

[2] Miller 3rd, M., Stineman, C., Vance, J., West, D., and Hall, I. 1997. The cytotoxicity of copper (II) complexes of 2-acetyl-pyridyl-4N-substituted thiosemicarbazones, *Anticancer Res. 18*, 4131-4139.

[3] Miller, M., Stineman, C., Vance, J., West, D., and Hall, I. 1999. Multiple mechanisms for cytotoxicity induced by copper (II) complexes of 2-acetylpyrazine-N-substituted thiosemicarbazones, *Appl. Organomet. Chem. 13*, 9-19.

[4] Petering, D. H., Loftsgaarden, J., Schneider, J., and Fowler, B. 1984. Metabolism of cadmium, zinc and copper in the rat kidney: the role of metallothionein and other binding sites, *Environ. Health Perspect. 54*, 73.

[5] Campana, M., Laborie, C., Barbier, G., Assan, R., and Milcent, R. 1991. Synthesis and cytotoxic activity on islets of Langerhans of benzamide thiosemicarbazone derivatives, *Eur. J. Med. Chem. 26*, 273-278.

[6] Uesugi, K., Sik, L. J., Nishioka, H., Kumagai, T., and Nagahiro, T. 1994. Extraction-spectrophotometric determination of palladium with 3-thiophenaldehyde-4-phenyl-3-thiosemicarbazone, *Microchem. J. 50*, 88-93.

[7] Singh, R., Garg, B., and Singh, R. 1978. Analytical applications of thiosemicarbazones and semicarbazones: A review, *Talanta 25*, 619-632.

[8] Khuhawar, M. Y., and Arain, G. M. 2006. Liquid chromatographic determination of vanadium in petroleum oils and mineral ore samples using 2-acetylpyridne-4-phenyl-3-thiosemicarbazone as derivatizing reagent, *Talanta 68*, 535-541.

[9] Tian, Y.-p., Duan, C.-y., Zhao, C.-y., You, X.-z., Mak, T. C., and Zhang, Z.-y. 1997. Synthesis, crystal structure, and second-order optical nonlinearity of Bis (2-chlorobenzaldehyde thiosemicarbazone) cadmium halides (CdL2X2; X= Br, I), *Inorg. Chem. 36*, 1247-1252.

[10] Yousef, T., Rakha, T., El Ayaan, U., and El Reash, G. A. 2012. Synthesis, spectroscopic characterization and thermal behavior of metal complexes formed with (Z)-2-oxo-2-(2-(2-oxoindolin-3-ylidene) hydrazinyl)-N-phenylacetamide (H_2OI), *J. Mol. Struct. 1007*, 146-157.

[11] Yousef, T., El-Reash, G. A., El-Gammal, O., and Ahmed, S. F. 2014. Structural, DFT and biological studies on Cu (II) complexes of semi and thiosemicarbazide ligands derived from diketo hydrazide, *Polyhedron 81*, 749-763.

[12] Stoica, L., Dinculescu, M., and Plapcianu, C. G. 1998. Mn (II) recovery from aqueous systems by flotation, *Water Res. 32*, 3021-3030.

[13] Vogel, A. I. 1991. *Vogel'sTextbook of Quantitative Chemical Analysis*, 5th ed., Longmans, London.

[14] Patai, S. 1970. *chemistry of the carbon-nitrogen double bond*, Interscience, NewYork.

[15] Hawkey, P., and Lewis, D. 1994. *Medical Bacteriology—A Practical Approach*, Oxford University Press, United Kingdom.

[16] Mosmann, T. 1983. Rapid colorimetric assay for cellular growth and survival: application to proliferation and cytotoxicity assays, *J. Immunol. Methods 65*, 55-63.

[17] Mauceri, H. J., Hanna, N. N., Beckett, M. A., Gorski, D. H., Staba, M.-J., Stellato, K. A., Bigelow, K., Heimann, R., Gately, S., and Dhanabal, M. 1998. Combined effects of angiostatin and ionizing radiation in antitumour therapy, *Nature 394*, 287-291.

[18] Delley, B. 2002. Hardness conserving semilocal pseudopotentials, *Phys. Rev. B: Condens. Matter 66*, 155125.

[19] Modeling and Simulation Solutions for Chemicals and Materials Research, Materials Studio, *Version 7.0*, Accelrys software Inc., San Diego, USA (2011).

[20] Hehre, W. J. 1986. *Ab initio molecular orbital theory*, Wiley-Interscience.

[21] Kessi, A., and Delley, B. 1998. Density functional crystal vs. cluster models as applied to zeolites, *Int. J. Quantum Chem 68*, 135-144.

[22] Matveev, A., Staufer, M., Mayer, M., and Rösch, N. 1999. Density functional study of small molecules and transition-metal carbonyls using revised PBE functionals, *Int. J. Quantum Chem 75*, 863-873.

[23] Hammer, B., Hansen, L. B., and Nørskov, J. K. 1999. Improved adsorption energetics within density-functional theory using revised Perdew-Burke-Ernzerhof functionals, *Phys. Rev. B: Condens. Matter 59*, 7413-7421.

[24] El-Gammal, O. A., El-Reash, G. A., and Ahmed, S. F. 2012. Structural, spectral, thermal and biological studies on 2-oxo-N′-((4-oxo-4H-chromen-3-yl) methylene)-2-(phenylamino) acetohydrazide (H 2 L) and its metal complexes, *J. Mol. Struct. 1007*, 1-10.

[25] El-Ayaan, U., Kenawy, I., and El-Reash, Y. A. 2007. Synthesis, thermal and spectral studies of first-row transition metal complexes with Girard-T reagent-based ligand, *J. Mol. Struct. 871*, 14-23.

[26] Souza, P., Sánchez-Kaiser, F., Masaguer, J. R., and Arquero, A. 1987. Complexes of chromium (III), cobalt (II) and copper (II) with sulphur or oxygen and nitrogen donors, *Transition Met. Chem. 12*, 128-130.

[27] Maurya, R., Mishra, D., Jaiswal, S., and Dubey, J. 1995. Synthesis, Magnetic and Spectral Studies of Some Novel Mixed-Ligand Cyanonitrosyl {MnNO} 6 Complexes of Manganese (I) with Potentially Mono-, Biand Tri-Dentate Pyridine Derivatives, *Synth. React. Inorg. Met.-Org. Chem. 25*, 521-535.

[28] Tossidis, I., Bolos, C., Aslanidis, P., and Katsoulos, G. 1987. Monohalogeno benzoylhydrazones III. Synthesis and structural studies of Pt (II), Pd (II) and Rh (III) complexes of Di-(2-pyridyl) ketonechlorobenzoyl hydrazones, *Inorg. Chim. Acta 133*, 275-280.

[29] Joseyphus, R. S., Dhanaraj, C. J., and Nair, M. S. 2006. Synthesis and characterization of some Schiff base transition metal complexes derived from vanillin and L (+) alanine, *Transition Met. Chem. 31*, 699-702.

[30] Moore, J. W., and Pearson, R. G. 1961. *Kinetics and mechanism*, John Wiley & Sons, New York.

[31] Hatakeyama, T., and Quinn, F. 1994. Fundamentals and applications to polymer science, *J. Therm. Anal.*

[32] Maravalli, P., and Goudar, T. 1999. Thermal and spectral studies of 3-N-methyl-morpholino-4-amino-5-mercapto-1, 2, 4-triazole and 3-N-methyl-piperidino-4-amino-5-mercapto-1, 2, 4-triazole complexes of cobalt (II), nickel (II) and copper (II), *Thermochim. Acta 325*, 35-41.

[33] Yusuff, K. M., and Sreekala, R. 1990. Thermal and spectral studies of 1-benzyl-2-phenylbenzimidazole complexes of cobalt (II), *Thermochim. Acta 159*, 357-368.

[34] Siddalingaiah, A. H. M., and Naik, S. G. 2002. Spectroscopic and thermogravimetric studies on Ni(II), Cu(II) and Zn(II) complexes of di(2,6-dichlorophenyl)carbazone, *J. Mol. Struct. THEOCHEM 582*, 129-136.

[35] Chacko, J., and Parameswaran, G. 1984. Thermal decomposition kinetics of vanillidene anthranilic acid complexes of cobalt (II), nickel (II), copper (II) and zinc (II), *J. Therm. Anal. Calorim. 29*, 3-11.

[36] El-Gammal, O. A. 2010. Synthesis, characterization, molecular modeling and antimicrobial activity of 2-(2-(ethylcarbamothioyl) hydrazinyl)-2-oxo-N-phenylacetamide copper complexes, *Spectrochimica Acta Part A: Molecular and Biomolecular Spectroscopy 75*, 533-542.

[37] Despaigne, A. A. R., Da Silva, J. G., Do Carmo, A. C. M., Piro, O. E., Castellano, E. E., and Beraldo, H. 2009. Copper (II) and zinc (II) complexes with 2-benzoylpyridine-methyl hydrazone, *J. Mol. Struct. 920*, 97-102.

[38] West, D. X., Swearingen, J. K., Valdés-Martínez, J., Hernández-Ortega, S., El-Sawaf, A. K., van Meurs, F., Castiñeiras, A., Garcia, I., and Bermejo, E. 1999. Spectral and structural studies of iron (III), cobalt (II, III) and nickel (II) complexes of 2-pyridineformamide N (4)-methylthiosemicarbazone, *Polyhedron 18*, 2919-2929.

[39] El-Gammal, O., Bekheit, M., and Tahoon, M. 2015. Synthesis, characterization and biological activity of 2-acetylpyridine-α-naphthoxy acetylhydrazone its metal complexes, *Spectrochimica Acta Part A: Molecular and Biomolecular Spectroscopy 135*, 597-607.

[40] Govindarajan, M., Periandy, S., and Carthigayen, K. 2012. FT-IR and FT-Raman spectra, thermo dynamical behavior, HOMO and LUMO, UV, NLO properties, computed frequency estimation analysis and electronic structure calculations on α-bromotoluene, *Spectrochim. Acta. A Mol. Biomol. Spectrosc. 97*, 411-422.

[41] Abu El-Reash, G. M., El-Gammal, O., Ghazy, S., and Radwan, A. 2013. Characterization and biological studies on Co (II), Ni (II) and Cu (II) complexes of carbohydrazones ending by pyridyl ring, *Spectrochim. Acta. A Mol. Biomol. Spectrosc. 104*, 26-34.

[42] Pearson, R. G. 1989. Absolute electronegativity and hardness: applications to organic chemistry, *J. Org. Chem. 54*, 1423-1430.

[43] Padmanabhan, J., Parthasarathi, R., Subramanian, V., and Chattaraj, P. 2007. Electrophilicity-based charge transfer descriptor, *J. Phys. Chem. A 111*, 1358-1361.

[44] Vogel, A. I. 1994. *A Text Book of Quantitative Inorganic Analysis*, Longmans, London.

[45] Ghazy, S. E.-S., Samra, S. E.-S., Mahdy, A. E.-F. M., and EL-MORSY, S. M. 2006. Removal of aluminum from some water samples by sorptive-flotation using powdered modified activated carbon as a sorbent and oleic acid as a surfactant, *Anal. Sci. 22*, 377-382.

[46] Klassen, V. I., and Mokrousov, V. A. 1963. *An introduction to the theory of flotation*, Butterworths.

[47] Ghazy, S. E.-S., and Moustafa, G. A.-H. 2001. Flotation-Separation of Chromium (VI) and Chromium (III) from Water and Leathers Tanning Waste Using Active Charcoal and Oleic Acid Surfactant, *Bull. Chem. Soc. Jpn. 74*, 1273-1278.

[48] Ghazy, S. E., and Kabil, M. A. 1994. Determination of Trace Copper in Natural Waters after Selective Separation by Flotation, *Bull. Chem. Soc. Jpn. 67*, 2098-2102.

[49] Ghazy, S., Rakha, T., El-Kady, E., and El-Asmy, A. 2000. Use of some hydrazine derivatives for the separation of mercury (II) from aqueous solutions by flotation technique, *Indian J. Chem. Technol. 7*, 178-182.

[50] Pol'kin, S., Berger, G., Revazashavili, I., and Shchepkina, M. 1968. Phase diagram and collector properties of oleic acid with changing pH, *Izv. Vyssh. Ucheb. Zaved., Tsvet. Met 11*, 6-11.

[51] Ramachandra, R. 1982. Surface chemistry of froth flotation, Vol. 2, Reagents and Mechanisms, Kluwer Academicy Plenum Publishers, New York.

Access this Article in Online	
	Website: www.ijarbs.com
	Subject: Chemistry
Quick Response Code	

How to cite this article:
Magdy M. Khalifa, Hany M. Youssef, Abdulnasir A. Majeed, Gaber M. Abu El-Reash. (2016). Structural investigation, biological and flotation studies of Co(II) and Zn(II) complexes of salicoyl hydrazone ending by thiazole ring.. Int. J. Adv. Res. Biol. Sci. 3(6): 235-254.